Korean Journal of Geomatics
Vol. 3, No. 2 / March 2004
pp. 141~148

On the Crustal Deformation Study Using Permanent GPS Stations in Korean Peninsula

Hong-Sic YUN* and Jae-Myoung CHO**

Abstract

This paper deals with the characteristics of strain pattern by using permanent GPS stations in Korea in terms of seismic activity and tectonics. Fourteen GPS stations involved in precise baseline vector solution and horizontal strain components were calculated using the differences of mean baseline from ten daily solutions during the time span of three years. The mean rate of maximum shear strain is 0.12 μ/yr. The mean direction of principal axes of the compression is about 85° N.

Keywords : *Maximum shear strain, Seismicity, Permanent GPS station, Baseline vector, Focal mechanism*

1. Introduction

The Korean peninsula has experienced no destructive earthquake except a few very slightly damaging earthquakes since the end of the 18th century. It is therefore widely believed that the Korean peninsula is geologically stable and free form earthquake hazards. This is the reason that there has been little concern about the crustal movement in Korea. In historical documents, however, such as Samkook Sakie, Chosun Wangjo Silrock, many destructive earthquakes were recorded, especially in 6^{th}~7^{th}, 13^{th} and 16^{th}~18^{th} centuries (Kim and Shu, 1977). They remarked that steady accumulation of crustal strain and its sudden release by earthquakes occurred repeatedly in the Korean peninsula during those times.

In Korea, National Geography Institute (NGI) has utilized satellite surveying techniques since 1979. Satellite surveying has been performed at Pusan, Kyeongju and Cheju Island using two Magnavox 1502 receivers through cooperation with Geodetic Surveyor Institute of Japan until 1982. Twenty islands have been utilized for Transit Satellite observations as of 1991.

Since 1991, NGI has used GPS receivers to strengthen the PPGN and the Precise Secondary Geodetic Network. NGI has established fourteen permanent GPS sites in a continuously operating reference station network starting with the first station called SUWN using a Turborogue^{TM} SNR-8000 receiver on 15 March 1995. Currently, sixty permanent GPS sites operated by other government agencies established for the purpose of cadastral surveying, geodynamic application and atmospheric research.

During 1996 and early 2000, NGI established a national network of permanently installed, continuously observing, automatically communicating GPS stations in all parts of Korea - the active stations of the National GPS Network. The complete network includes about seventy-four active stations, of which fourteen are owned by NGI, and the remainder operated by other government agencies working in partnership with NGI. Fig. 1 shows the typical type of permanent GPS station established by NGI.

The active stations are deployed such that any point in Korea, including Cheju island, will be within 30km of the nearest active station. The active stations are installed with dual-frequency geodetic quality receivers, mostly with choke ring antennae to minimize the effects of multi-path on a ground plane. Each site collects data at 30seconds epoch and communicates

*Assistant Professor, Department of Civil and Environmental Engineering, Sungkyunkwan University (E-mail : yhs@geo.skku.ac.kr)
**Ph. D. Candidate, Department of Civil and Environmental Engineering, Sungkyunkwan University (E-mail : jmcho@geo.skku.ac.kr)

The manuscript for this paper was submitted for review on February 25, 2004 / accepted on May 25, 2004

Fig. 1. Typical type of permanent GPS station established by National Geography Institute.

data automatically by a ISDN/PSTN lines to NGI's master control center. This central computer downloads data from each station every hour and monitors the health of the system. At NGI, data are validated, converted to RINEX format and processed using Berness software. All the Korean GPS fiducial network receivers are remotely controlled from SUWN master station.

The daily acquisitions of the Korean GPS fiducial network are checked and archived at SUWN. A data quality check, using the UNAVCO QC v3 software is done periodically in order to verify the correct functionality of the Korean GPS fiducial network receivers. Daily precise ITRF97 coordinates of all active stations are computed weekly by NGI and used to monitor the positional stability and data quality of each station. Yun (2000) performed a time series analysis of SUWN site. NGI (2001) announced the official coordinates of fourteen active stations referred to ITRF97.

This allows the study of data processing and present the general trend of strain that obtained from GPS observations. We also discuss the characteristics of general strain patterns in terms of geological and tectonic settings in and around the Korean peninsula.

2. Tectonic Environment and Seismic Activates in and around the Korean peninsula

The Korean peninsula is 200~300km wide and ~ 1,000 km long from north to the south, protruding from the eastern part of the Eurasian continent (Fig. 2). The Korean peninsula extends southward from northeast Asia and has a close affinity with the Asian continent, especially with the Northeast China paraplatform, in geological and tectonic setting. Korea is a hilly country, about 70% of the territory is mountainous with an average height of about 480m. The wire frame expression of the topography is presented in Fig. 3.

In this study, we treat the area south of the 38° N parallel. In this area, the major mountain range, Taeback Range runs in the direction of NNE-SSW

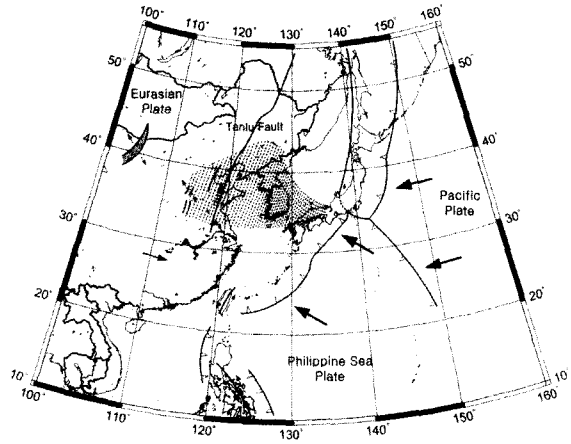

Fig. 2. Tectonic environment in and around the Korean peninsula.

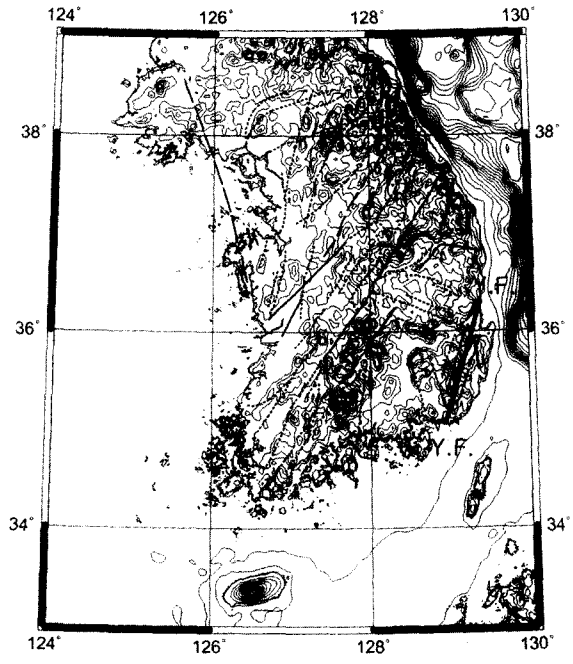

Fig. 3. Topographic map generated from 1″ DEM and lineament map of the southern part of the Korean peninsula from the original map by Korean Energy Resource Institute (1993).

along the east coast. In the central part, Soback mountain range trend parallel to the Taeback range. The direction of NNE-SSW is characteristic in the topography of Korea.

The trend of NNE-SSW is also recognized in the direction of the geological lineaments in Korea. Fig. 3 shows the lineaments compiled from the map after Korea Energy Resource Institute (1993). The Yangsan fault, denoted by Y.F., is the most remarkable fault in the southeastern part. Along the Yangsan fault, Quaternary formations are developed in many places from the valley side to the lineament center. Otsuki and Ehiro (1978) asserts the Yangsan fault which was active in Tertiary has reactivated recently as a right-lateral fault. At present, the Yangsan fault is the only active fault in Korea.

In the Korean peninsula, the first earthquake observation with seismographs was started at Incheon in 1905. Seismograph stations had increased to six at the end of 1930s in Pusan, Taegu, Incheon, Seoul, Pyongyang and Chupungryong (Lee and Jung, 1980). Because these stations are located nearly along a line, the epicenter is obtained from the data of International Seismological Center (ISC), as one World-Wide Standard Seismograph Network (WWSSN) station has been in operation in Seoul since 1963.

Fig. 4 shows the spatial distribution of the earthquake ($mb \geq 4.5$) in and around the Korean peninsula during the period 1964 ~ 1990 from ISC data. Though numbers of the earthquakes are limited, there is a tendency that seismicity is relatively high in the vicinity of the southeastern coast of the peninsula.

Focal mechanism solutions of the earthquakes in Fig. 5 were obtained by Jun (1990) as shown in Fig. 5 by analyzing moment tensors. Except one earthquake of normal fault type in the northern peninsula, all the earthquakes show the mechanisms of strike slip fault type with small thrust components, the P-axis of which are nearly horizontal and trend NEE-SWW. This is

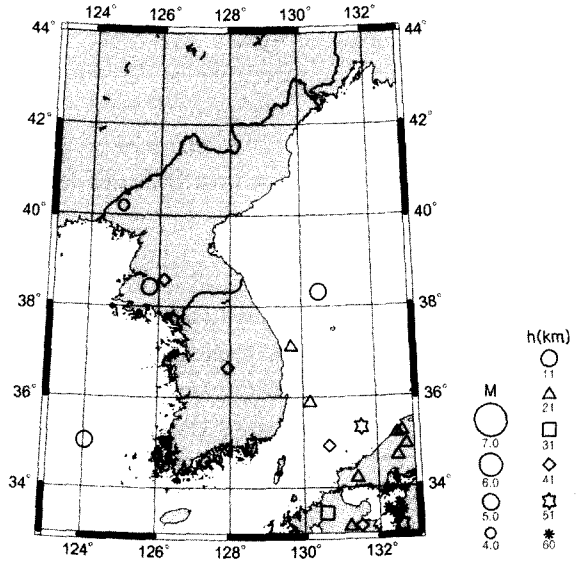

Fig. 4. Epicentral distribution of earthquakes($mb \geq 4.5$) in and around the Korean peninsula from the data of ISC.

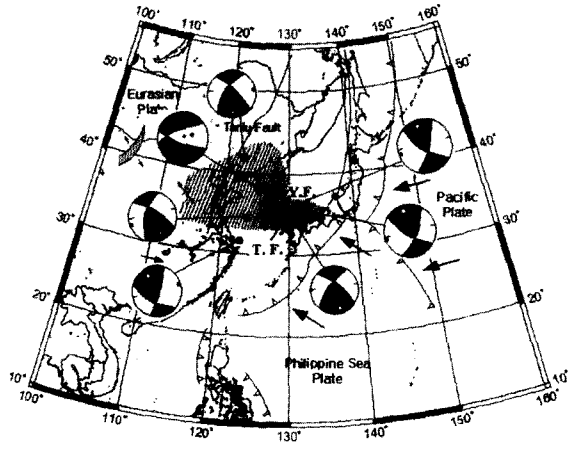

Fig. 5. Focal mechanism of earthquakes in and around the Korean peninsula (after Jun, 1990). Empty and full small circles in the focal sphere represent T and P axis, respectively.

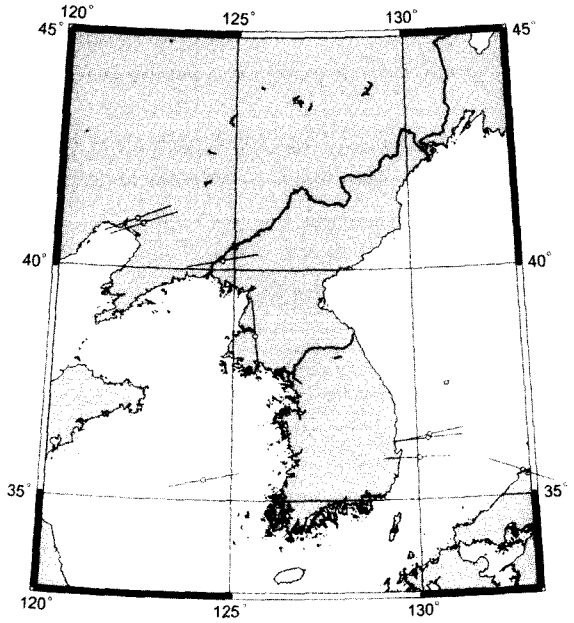

Fig. 6. Horizontal projection of P-axis of focal mechanisms of the earthquakes in and around the Korean peninsula (after Jun, 1990).

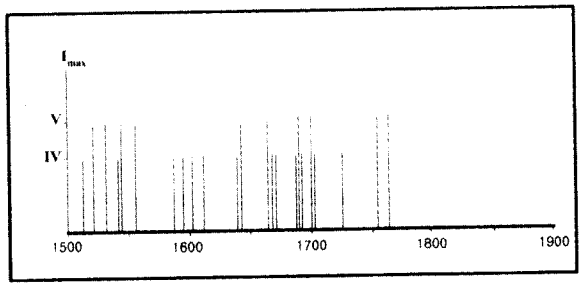

Fig. 7. Frequency distribution of damaging earthquakes in the Korean peninsula during the period from 1500 to 1900 (after Choi and Sato, 1995). Imax denotes the maximum intensity in JMA scale.

considered as a characteristic of the earthquakes in this region.

Through present seismicity in the Korean peninsula is not high, many destructive earthquakes have been recorded in historical documents of Korea. For example, the earthquake of 779 A.D. killed more than 100 people in Kyungju and the earthquake of 1643 caused large tsunami and serious damage to the east coast of southern peninsula. Richter (1958) remarked that earthquake activity was high during the period from the 16th to the 18th centuries in the Korean peninsula. The first synthetic investigations on record are Samkook Sakie, Koryosa and Chosun Wangjo Silrock. They compiled a list fo damaging earthquakes from 2 A.D. to 1905, and evaluated their intensity in the JMA scale. Since then, some researches on the seismicity activity in historical times has been made in terms of the geological structure of the Korean peninsula (e.g. Lee, 1985).

The reign system of the Chosun Dynasty (1400~1900) was centralized and the communication between the capital and province was developed. It is likely, therefore, that most of the destructive earthquakes in the time of the Chosun Dynasty were recorded. We examined closely the chronicles of the Chosun Dynasty, Wangjo Silrock, and compiled the catalogue of destructive earthquakes during the period from 1400 to 1900 (Choi and Sato, 1995). In the chronicles, twenty-three destructive earthquakes were recorded during the period from 1500 to 1760 as shown in Fig. 7. No damaging earthquake occurred in the period 1761~1900, making a marked contrast to the active seismicity during the previous period.

3. GPS Data Analysis Using the GIPSY/OASIS II Software

In this study the GPS network is composed of fourteen stations that are SUWN, WNJU, KANR, SEOS, DAEJ, SNJU, TABK, WULJ, JUNJ, TEGN, KNJU, KWNJ, JINJ, and CHJU stations chosen from existing permanent GPS stations. They all equipped with Trimble 4000SSI receivers with choke-ring antenna. Each of the analyzed fourteen stations has at least 3 years of continuous data. We decimated pseudo-range and phase data to 300 seconds samples and used 15° elevation cutoff angle.

The data were analyzed using the GIPSY-OASIS (GPS-Inferred Positioning System and Orbit Analysis Simulation Software) II developed at Jet Propulsion Laboratory (JPL) of the California Institute of Technology. The GIPSY-OASIS II has been used extensively during the last few years to analyze GPS carrier phase and pseudo-range data from many experiments yielding baseline precisions at the level of a few parts in 10^9 or better (Lichten and Border, 1987; Stephen et al., 1996). Overviews of the GIPSY-OASIS II are given in Lichten and Border (1987) and Blewitt (1989).

For the solution of baseline vectors we designed the triangulation network which consist of fourteen stations as shown in Fig. 9. One baseline was allocated to each ten day and ten daily solutions were computed for each baseline. Allocation of one baseline per ten days ensured that separate baseline solutions were independent. Due to the long baselines the final GPS solutions are computed using a linear ionosphere-free combinations of L1 and L2 observable and the double difference processing technique associated with the JPL precise ephemeredes was used to determine the baseline vectors. Wet tropospheric delay effects are modeled using a random walk stochastic processed discussed in (Dodson et al., 1996). The computation models closely follow the IERS Standards (McCarthy, 1992).

Data processing started with the automatic editing of the GPS data. This included elimination of bad data points and cycle slip detection and repair, when possible. In pre-processing of GPS data we performed the review and cataloging of collected data files, processing phase measurements to determine baseline vectors and/or unknown positions, and performing both adjustments and transformations to the processed vectors and positions. We also analyzed quality control using statistical measures and professional judgment to achieve the desired level of confidence. Ten days

Table 1. Ten day mean baseline length and differences between 1999 and 2002

Baselines	1999 Mean baseline (m)	2002 Mean baseline (m)	Differences (mm)
CHJU - JINJ	231132.0109±0.00031	231132.0113±0.00026	-0.4
CHJU - KWNJ	187917.8628±0.00044	187917.8634±0.00045	-0.6
CHJU - SEOS	361919.2537±0.00031	361919.2556±0.00032	-2.0
DAEJ - JUNJ	65347.4088±0.00023	65347.4094±0.00027	-0.6
DAEJ - SEOS	89194.3056±0.00051	89194.3144±0.00042	-0.9
DAEJ - SNJU	69120.3952±0.00029	69120.3876±0.00031	-0.8
DAEJ - SUWN	101333.2169±0.00033	101333.2207±0.00036	-0.4
DAEJ - WNJU	115920.1119±0.00027	115920.1073±0.00029	-4.6
JINJ - JUNJ	111424.6179±0.00031	111424.6183±0.00038	-0.4
JINJ - KNJU	137374.7167±0.00030	137374.7187±0.00058	2.0
JINJ - KWNJ	103795.8338±0.00038	103795.8315±0.00028	2.4
JINJ - TEGN	106170.2668±0.00030	106170.2671±0.00031	-0.2
JUNJ - KWNJ	76558.879±0.00030	76558.8774±0.00032	2.2
JUNJ - SEOS	118450.1622±0.00036	118450.1627±0.00045	-0.6
JUNJ - SNJU	108592.3584±0.00034	108592.3600±0.00036	1.5
JUNJ - TEGN	150684.0138±0.00054	150684.0157±0.00055	1.9
KANR - TABK	68379.0031±0.00038	68379.0007±0.00051	2.4
KANR - WNJU	94563.0816±0.00043	94563.0821±0.00053	-0.5
KANR - WULJ	99003.1330±0.00023	99003.1322±0.00028	0.9
KNJU - TEGN	57240.6785±0.00042	57240.6742±0.00038	-4.3
KNJU - WULJ	139623.9789±0.00054	139623.9770±0.00061	-1.9
KWNJ - SEOS	181237.1117±0.00042	181237.1134±0.00043	-1.7
SEOS - SUWN	74507.4277±0.00051	74507.4264±0.00043	1.3
SNJU - TABK	114161.4085±0.00032	114161.4157±0.00034	-7.2
SNJU - TEGN	79086.8160±0.00027	79086.8165±0.00022	-0.5
SNJU - WNJU	107767.1900±0.00026	107767.1903±0.00029	-0.3
SNJU - WULJ	132205.1233±0.00052	132205.1247±0.00037	-1.4
SUWN - WNJU	79450.3951±0.00026	79450.3950±0.00025	0.2
TABK - WNJU	93332.7283±0.00042	93332.7354±0.00043	-7.1
TABK - WULJ	43182.9312±0.00033	43182.9281±0.00034	3.1
TEGN - WULJ	132341.5336±0.00041	132341.5374±0.00024	-3.9

baseline length and difference between 1999 and 2002 are listed in Table 1.

We could calculate horizontal strains from the differences of the mean baseline vectors of ten daily solutions between the time span of three years, if they had enough accuracy for the present strain calculation.

4. Strain Calculation

In the present study, we have used the formula of 2-dimensional infinitesimal strain. As there is a confusion in the expression of the strain (Okada, 1981), we present here the formula after Jeager (1964). We consider here 2-dimensional elastic deformation of x-y plane. Let the point P' and Q' in Fig. 8 be the displaced points of P and Q due to the elastic deformation, respectively. The x and y components of the displacement of Q' written as uQ and vQ are expressed as follows:

$$u_Q = u_P + \frac{\partial u}{\partial x} dx + \frac{\partial u}{\partial y} dy \quad (1)$$

$$v_Q = v_P + \frac{\partial v}{\partial x} dx + \frac{\partial v}{\partial y} dy \quad (2)$$

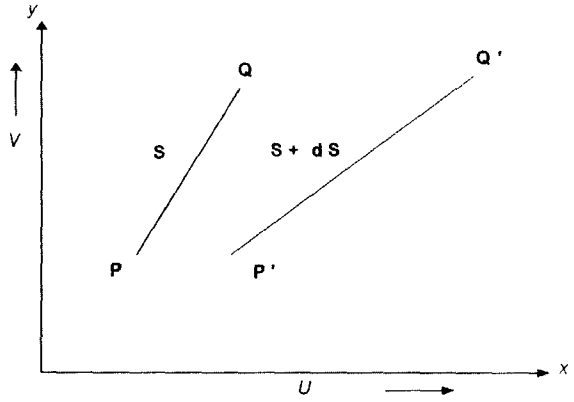

Fig. 8. Displacements of the two points P and Q on the x-y plan due to the elastic deformation

where $\frac{\partial u}{\partial x} = E_x$, $\frac{\partial v}{\partial y} = E_y$, $\frac{\partial v}{\partial x} + \frac{\partial u}{\partial y} = \gamma_{xy}$

The principal axes of strain ε_1 and ε_2 are given by:

$$\varepsilon_{1,2} = \frac{E_x + E_y}{2} \pm \sqrt{\left(\frac{E_x - E_y}{2}\right)^2 + \left(\frac{\gamma_{xy}}{2}\right)^2} \quad (3)$$

with direction θ and $\theta + \pi/2$, with θ given by:

$$\tan 2\theta = \frac{\gamma_{xy}}{E_x - E_y} \quad (4)$$

By convention, extension is positive, $\varepsilon_1 > \varepsilon_2$, and the principal shortening axis is oriented at an azimuth θ measured clockwise from north.

The maximum shear strains in the x-y plane are associated with axes at 45° to the directions of the principal strains. The algebraically maximum shear strain is given by the following equation:

$$\frac{\gamma_{max}}{2} = \sqrt{\left(\frac{E_x - E_y}{2}\right)^2 + \left(\frac{\gamma_{xy}}{2}\right)^2} \quad (5)$$

$$\gamma_{max} = \pm 2\sqrt{\left(\frac{E_x - E_y}{2}\right)^2 + \left(\frac{\gamma_{xy}}{2}\right)^2} = \pm(\varepsilon_1 - \varepsilon_2) \quad (6)$$

Our GPS results show that the strain rate field is dominated by an compressional component of -0.004 μ/yr (dilatation) and maximum shear strain γ_{max} of 0.122 μ/yr.

Table 2 is listed the results of the present strain calculation. Fig. 9 shows the result of the present study of the horizontal crustal strains in Korea, in which lengths and directions of facing pair arrows represent rate of γ_{max} and azimuth of ε_2, respectively. This is the first figure that represents the general feature of

Table 2. The First result of strain calculation from GPS observations in Korea

Number	ε_1 (μ/yr)	ε_2 (μ/yr)	Directions (degree)	γ_{max} (μ/yr)	Δ (μ/yr)
1	0.098	-0.0236	61.476	0.1216	0.0744
2	0.0641	-0.0504	45.49	0.1145	0.0137
3	0.002	-0.1142	100.323	0.1162	-0.1121
4	0.0941	0.0014	104.086	0.0927	0.0954
5	0.0767	-0.0578	73.691	0.1345	0.019
6	-0.009	-0.2006	119.603	0.1917	-0.2096
7	0.098	-0.0782	75.924	0.1762	0.0198
8	0.1274	-0.0563	84.042	0.1837	0.0712
9	0.041	-0.112	81.13	0.153	-0.0713
10	0.0324	0.0028	74.764	0.0296	0.0353
11	0.0779	-0.0309	84.008	0.1089	0.047
12	0.1517	-0.0222	95.793	0.1739	0.1295
13	0.0343	-0.1904	51.131	0.2248	-0.1561
14	0.0132	0.0046	114.529	0.0086	0.0178
15	0.0039	-0.0428	80.299	0.0466	-0.0389
16	0.012	-0.0074	91.11	0.0194	0.0046
17	0.0185	-0.108	84.92	0.126	-0.089
18	0.1294	-0.047	111.326	0.1765	0.0824
Mean	0.0592	-0.0629	85.203	0.1221	-0.0037

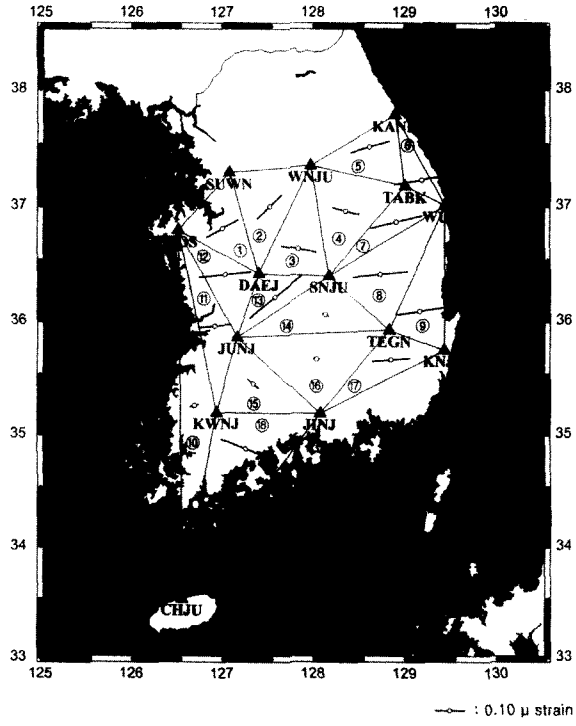

Fig. 9. Distribution of earth strain in Korea obtained by the present study. Length and direction of facing arrows represent the rate of maximum shear strain γ_{max}, and the azimuth of principal axis of compression.

crustal strain obtained from GPS observations in Korea. It is remarkable in Fig. 8 that the dominant trend of the principal axis of the maximum compression strain (ε_2) is NEE-SWW (about 85°). The general characteristic of the field is a bi-axial compression. The largest maximum shear strain that occur inside the network is about 0.22 μ/yr.

This mean rate of maximum shear strain is nearly one third of the mean rate of Japan deduced from the data of the revision survey of the first order triangulation net (Sato, 1973). The GPS network composed of fourteen stations in Korea shows localized deformation with maximum shear oriented NNE-SSW and compression deformation from negative dilatation.

5. Conclusions

The main characteristics of the strain change during the three years in Korea obtained from the present study are revealed that the mean rate of the maximum shear strain change is 0.122 μ/yr and the direction of the principal axis is about 85°. The mean rate of dilatation is also -0.004 μ/yr.

Let us consider the relationship of these characteristics with other geo-scientific evidences. Jun (1990) showed in Fig. 4 that the horizontal projection of P-axis of the focal mechanisms of the earthquakes is NEE-SWW in and around the Korean peninsula, except one quake near the west coast of the peninsula.

Hence, the strain field shown in Figure 8 is consistent with the stress field deduced from earthquakes. Such principal axes are also concordant with the trend of faults and geological lineaments in Fig. 2, when Coulomb-Mohrs criterion for fracture (Scholz, 1990) is taken into account. In the case of fractures caused by compression stress, the fracture angle between the principal axis and the fracture plan is given as follow;

$$\tan 2\psi = (1/\kappa)$$

where ψ and κ are the fracture angle and coefficient of internal friction of rock, respectively. When κ is 0.5, ψ=32°. According to Jeager (1964) this is usually the case with rock fractures under the compression stress.

Sato(1973) estimated that the rate of secular change of γ_{max} is 0.1 μ/yr in the Chugoku district, southwest Japan, Where seismic activity is relatively low. This rate is nearly one third of mean rate of the Chubu disrict, central Japan, and is comparable with that of Korea. Jun(1990) suggested that Northeast China, Korean Peninsula and Chugoko district belong to the same seismo-tectonic zone as shown in Fig. 10. Taking the above into account, the mean rate of γ_{max} in Korea obtained by the present study is considered reasonable.

Fig. 10 shows the distribution of the P-axis in the western part of Honshu, Japan that the direction is NWW-SEE (Tsukahara and Kobayashi, 1991). Considering the relationship with the results of present

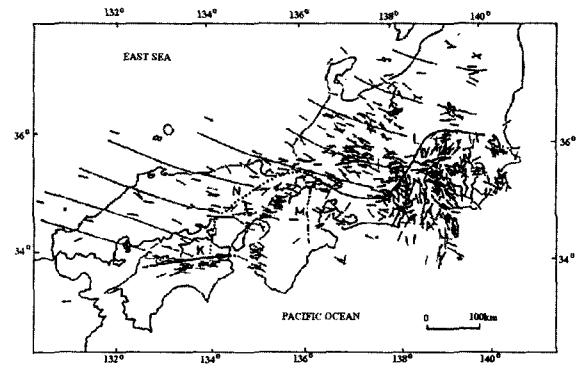

Fig. 10. Direction of the maximum compression stress of the Western part of Honshu, Japan, deduced from P-axis of earthquakes (after Tsukahara and Kobayashi, 1991).

research, there is a clear difference in the direction of the stress axis between the Korean peninsula and the East sea side of Chugoku district of Japan, notwithstanding the similarity in the seismicity and the strain rate in the both areas. This gives a strong likelihood of the existence of a certain tectonic line between the southern part of the Korean peninsula and the Chugoku district, Japan.

As a conclusion, the result of present study as shown in Fig. 9 represents the characteristics of the horizontal deformation of the crust in Korea, and contributes to the research on the seismo-tectonics in the Korean peninsula.

Acknowledgements

This work was supported by Korea Research Foundation Grant(KRF-2000-0402-000).

GIPSY-OASIS II software was used to GPS data processing. The authors are grateful to the reviewers for their time and effort taken to review this manuscript.

References

1. Blewitt, G. (1989), Carrier Phase Ambiguity Resolution for the Global Positioning System Applied to Geodetic Baseline up to 2000km, Journal of Geophysical Research, 94: 10,187-10,293.
2. Choi, J. H. and Sato, H. (1995), Historical Damaging Earthquakes in the Korean peninsula, Zisinz, Vol. 48, pp. 483-486 (in Japanese).
3. Choi, J. H. (1998), Horizontal Strain of the Crust in Korea inferred from Geodetic Data, Earth Planets Space, Vol. 50, pp.629-634.
4. Dodson A. H., Shardlow, P. J., Hubbard, L. C. M., Elgered, G. and Jarlemark, P. O. J. (1996), Wet Tropospheric Effects on Precise Relative GPS Height Determination, Journal of Geodesy, Vol. 70, pp. 188-202.
5. Jeager, J. C. (1964), Elasticity, Fracture and Flow, Methuen, London.
6. Jun, M S (1990) Tectonic Implication of Shallow Earthquakes in and around the Korean peninsula, Journal of Uppsala University, Sweden, 285, 1-30.
7. Kim, O. J. and Shu, J. H. (1977), A study on the characteristics and causes of earthquakes in Korea, Journal of Korean Mineral and Mining Institute, Vol. 14, pp. 240-268 (in Korean).
8. Korean Energy Resource Institute (1993), Neo-Tectonic Study in and around the Korea peninsula, Kr-93-(B)-14.
9. Lee, K. H. and Jung, H. O. (1980), A study of Instrumental Data of Earthquakes in the Korean peninsula, Journal of Geological Society. Korea, Vol. 9, pp. 32-45.
10. Lee, K. H. (1985), Studies on the Seismic Risk of the Korean peninsula (1), Journal of Geological Society. Korea, Vol. 14, pp. 227-240.
11. Lichten, S. M. and Border, J. S. (1987), Strategies for High Precision GPS Orbit Determination. Journal of Geophysical Research, 92: 12,751-12,762.
12. McCarthy, D. D. (1992), IERS Standards, IERS Technical Note 13, Observatoire de Paris.
13. Okada, Y. (1981), Confusions on the Expressions in Strain Analysis, Zisinz, Vol. 34, pp. 148-152 (in Japanese).
14. Otsuki, K. and Ehiro, M. (1978), Major strike-slip Faults and their Bearing on Spreading in the Japan sea, Journal of Physical Earth, Suppl. 26, pp. 537-562.
15. Richter, C. F. (1958), Elementary Seismology, W. H. Freeman and Company.
16. Sato, H. (1973), A Study of Horizontal Deformation of the Crust associated with Destructive Earthquakes in Japan, Bull. Geogr. Surv. Inst. Vol. 19, pp. 89-130.
17. Scholz, C. H. (1990), The Mechanics of Earthquakes and Faulting, Cambridge University Press, pp. 12-16.
18. Stephen, M. L., Sever, Y., Bertiger, W. L., Heflin, M., Hurst, K., Muellerschoen, R. J., Wu, S. C., Yunk, T. and Zumberge, J. (1996), GIPSY-OASIS II: A High Precision GPS Data Processing System and general Satellite Orbit Analysis Tool, Jet Propulsion Laboratory, California Institute of Technology, Pasadena, CA.
19. Tsukahara, H. and Kobayashi, Y. (1991), Crustal Stress in the Central and Western part of Japan. Zisinz, Vol. 44, pp. 221-231 (in Japanese).
20. Yun, H. S. (2000), Stability Evaluation of Permanent GPS Site by Least Square Spectrum Analysis, Journal of the Korean Society of Surveying, Geodesy, Photogrammetry and Cartography, Vol. 18, No. 1, pp. 379-385 (in Korean).
21. National Geography Institute (2001), A Study on the Establishment of the Geocentric Coordinate System in Korea, Technical Report, National Geography Institute (in Korean).